Effect of Moisture Content during Preparation on the Physicochemical Properties of Pellets Made from Different Biomass Materials

Xuya Jiang,[a,b] Weidong Cheng,[a] Jianbiao Liu,[a,b] Hang Xu,[a,b] Donghong Zhang,[a,b] Yuankun Zheng,[a] and Hongzhen Cai [a,b,*]

The influence of moisture content was investigated relative to the pellet forming process and the pellet properties. Three different types of raw biomass (pine sawdust, corn straw, and peanut shell) were pelletized by hot pressing at different moisture levels (12%, 14%, and 16%) in a pellet mill with horizontal and ring type dies to investigate its physical property indexes of durability, pellet density, and combustion performance. The results of the study showed that pellet density and heating value were related to the moisture content. The maximum pellet density of the fuel pellets of sawdust, corn straw, and peanut shells was 1180 kg/m^3, 1220 kg/m^3, and 1130 kg/m^3, respectively. The drop resistance and deformation resistance of pine sawdust and corn straw decreased with increased moisture content, but peanut shell initially increased with the increase of moisture before decreasing. The comprehensive combustion index of corn straw (14.03) was the highest during the combustion performance analysis in comparison to sawdust (11.10) and peanut shell (10.00). Overall, the optimal moisture content of sawdust, corn straw, and peanut shell was 12%, 12%, and 14%, respectively, and the combustion performance of the pellets made from corn straw was superior compared to the other two feedstocks.

Keywords: Biomass pellet; Moisture content; Hot press; Physical properties; Thermogravimetric

*Contact information: a: School of Agricultural Engineering and Food Science, Shandong University of Technology, Zibo 255000, China; b: Shandong Research Center of Engineering and Technology for Clean Energy, Zibo 255000, China; *Corresponding author: chzh666666@126.com*

INTRODUCTION

Currently, 80% of the total global energy demand is fulfilled by conventional fossil fuels (Guo *et al.* 2015). Global energy consumption was 1.53×10^8 GWh in 2010 and is predicted to increase up to 1.83×10^8 GWh 2.39×10^8 GWh between the years 2020 and 2040, respectively (Guo *et al.* 2015). Moreover, the constantly increasing use of fossil fuels has caused many environmental issues including air pollution and global warming (Bahrami and Abbaszadeh 2013). These problems can be overcome by producing cleaner renewable biofuels from abundantly available biomass. The annual global production of biomass is 1.2×10^{11} t, which can produce 6.11×10^8 GWh of energy (Guo *et al.* 2015). This energy is 3 to 4 times greater than current global energy demands (Guo *et al.* 2015).

In terms of energy consumption, China ranks the highest in the world. It is also the second largest importer of oil after the USA (Zhou *et al.* 2016b). Due to the extensive consumption of fossil fuels, China contributes to approximately 27.8% (10 billion tons) of total global carbon emissions (Zhou *et al.* 2016b). The use of biomass-based renewable energy is an attractive option for China due to the large availability of biomass, its

environmental benefits, as well as its cost effectiveness (Gu *et al.* 2019). China is an agriculturally based country and a huge amount of biomass is produced every year by different agricultural activities, which is equal to 460 million tons of standard coal per year (China National Energy Administration 2016). The major hindrances in the use of abundantly available biomass is its higher moisture contents, varying physical shapes, higher levels of dust, as well as its lower bulk density in comparison to fossil fuels, which makes it difficult for completing biomass transportation, handling, storage, and usage in its raw form. Moreover, the combustion performance of the raw biomass is also poor due to its higher moisture level, higher dust level, and lower bulk density (Khan *et al.* 2009; Saidur *et al.* 2011). Hence, increasing the bulk density of biomass is essential for ease of handling, transportation, and storage. The lower energy density of the biomass compared to conventional fossil fuels is also a challenge to its use as an alternative to conventional fossil fuels. These problems can be overcome by the pelletization of biomass (Kaliyan and Vance Morey 2009b). Biomass densification/pelletization will be helpful in reducing dust, uniformity of shape and size, decreasing the cost of storage and transportation, as well as improving thermal conversion (Demirbas 2004; Obernberger and Thek 2004; Gil *et al.* 2010; Verma *et al.* 2011; Li *et al.* 2012; Longhin *et al.* 2016; Bajwa *et al.* 2018; Trubetskaya *et al.* 2019).

The physical properties of the pellets, such as moisture contents, bulk density, porosity, durability, size, and hardness, are important indicators of their quality (Colley *et al.* 2006; Lam *et al.* 2008). Many researchers have studied the effect of moisture content on the physical properties of the biomass pellets (Colley *et al.* 2006) and concluded that the moisture content is an important factor that affects the quality of the biomass pellets. Tumuluru *et al.* (2011) studied the effect of the moisture contents of biomass on densification and concluded that higher moisture levels result in an increase in the contact area of the particles during densification by Van der Waals forces, decrease the glass transition temperature, and aid in the formation of a solid bridge. Mani *et al.* (2003) studied the effect of moisture on the densification process and concluded that the feedstock moisture acts as a binder during the biomass densification and increases the bonding of the particles through Van der Waals forces by increasing the contact area. Demirbas *et al.* (2004) studied the effect of moisture on the strength of pellets produced from spruce wood sawdust, and reported that when the moisture contents increased from 7% to 15%, the strength of the pellets also increased. Sokhansanj *et al.* (2005) studied the effect of moisture for pelletizing different types of materials and concluded that the optimum moisture content for pelleting the materials containing higher level of proteins (*i.e.*, animal feed) is 20% (w.b.); whereas for materials containing high levels of cellulose, the optimum moisture content for pelletizing the biomass is approximately 8% to 12% (w.b.).

In the above studies, the optimum moisture contents were found for the pelletization of biomass, and the effect of moisture was studied relative to physical properties. Moreover, in some of the studies, additives/binders were also used, which increased the concentration of pollutants during combustion (Florentino-Madiedo *et al.* 2018). The current study is the first time the authors studied and reported the optimum moisture content by hot pressing different biomass in a pellet mill with horizontal and ring type dies without adding any binder. Additionally, the physical, chemical, and thermal properties were analyzed, which provided comprehensive reference parameters to produce higher quality molding of fuel pellets. This study was intended to provide the foundation for subsequent research on the combustion and emission of pure material particles.

EXPERIMENTAL

Materials

Woody biomass (Pine sawdust (SD)), agricultural residues (corn straw (CS), and peanut shell (PS)) were used as feedstocks for the present study. All the feedstocks were collected from experimental fields of Shandong University of Technology, ZiBo, Shandong, China. These feedstocks were air-dried for one week after collection. The dried feedstocks were then crushed in a sieve mill (WN-300A; Xulang Machinery Equipment Co., Ltd., Guangzhou, China) using a 4-mm screen. The feedstocks were then stored at room temperature (25 °C) and ambient humidity (45 to 75%) in woven bags for further studies.

Methods

Proximate analysis

The moisture content (*M*) of all the samples was measured using a blast-drying oven (DHG-9420A; Yiheng Scientific Instrument Co., Ltd., Shanghai, China) according to the standard method GB/T 28731 (2012). The ash (*A*) and volatile matter (*V*) contents were determined using a muffle furnace (SX3-5-14; Yunyue Instrument Equipment Co., Ltd., Shanghai, China) according to the standard method GB/T 28731 (2012). The fixed carbon (FC) was measured by the difference according to the standard method GB/T 28731 (2012). For each of the analyses mentioned above, three replicate measurements were taken, and the average was reported.

Ultimate analysis

The carbon, hydrogen, nitrogen, and sulphur contents of the materials were determined simultaneously using an elemental analyzer (model EA300; Euro Vector, Pavia, Italy) according to the Chinese standard method JJG 017 (1996). Results from three measurements were averaged.

Heating value

The heating value (HV) of the materials was analyzed using a bomb calorimeter (model C2000; IKA, Staufen, Germany). A 1 g sample pellet was weighed using a digital balance within an accuracy of 0.0001 g. The sample was then placed in a crucible, and combustion of the sample was completed in a calorimeter to obtain the heating value, based on an average of three measurements.

Sample Preparation

Depending on the initial moisture content of the biomass found during the proximate analysis, the moisture contents of the biomass were adjusted to higher levels (12%, 14%, and 16%) by adding water according to the following Eq. 1,

$$x = m(k_2 - k_1) / (1 - k_2) \quad (1)$$

where x is the mass (kg) of water required to be added, m is the initial mass (kg) of material, and k_1 and k_2 are the initial and targeted moisture content (%) of materials, respectively.

After calculating the mass of water to be added in the biomass to be adjusted at suitable levels, the biomass was blended with water in a mixer (JHX-1-5; Jintai Material Co., Ltd., Zhengzhou, China) until the homogeneous mixture of biomass was formed.

Pelletization Process

The biomass pellets were fabricated without a binder in a pellet mill with horizontal and ring type dies with 8-mm die holes (Type 470; Jinan Taichang Transmission Machinery Co., Ltd., Jinan, China), as shown in Fig. 1. The specifications of the machine are presented in Table 1.

Fig. 1. Biomass pellet mill with horizontal and ring type die

Table 1. Specifications of the Molding Equipment

Specification	Parameter/Value	Measurement Unit
Electric motor rated power	5.5	kW
Electric motor supply voltage	380	V
Motor rotational speed	1480	r/min
Productivity	0.7 to 1	t/h
Diameter of the press rollers	200	mm
Width of the press rollers	10	mm
Type of die	Ring mold	-
Thickness of the die	70	mm
Diameter of the holes in the die	8	mm
Dimensions of the pellet mill	2200 × 1000 × 1500	mm
Mass of the pellet mill	5.5	ton
Molding temperature	90 ± 10	°C
Cone angle	50	°
Transmission ratio	18	-

Physical Properties of Biomass Fuel Pellets

The physical properties mainly included durability and pellet density.

Microstructure

The microstructure of the feedstocks was analyzed using a field emission scanning electron microscope (FE-SEM) (Quanta 250; FEI Company, Hillsboro, OR, USA).

Pellet density

The diameter and length of the pellets were measured with a Vernier caliper within an accuracy of 0.01 mm, and the mass was measured using a digital balance within an accuracy of 0.0001 g. The measurements were done in triplicates and the average results

were used. The pellet density of the fuel pellets was determined using Eq. 2 (Wang *et al.* 2018a),

$$\rho = 4m / (\pi D^2 L) \quad (2)$$

where ρ is the pellet density (kg/m^3), m is the mass (kg) of a single pellet, D is the diameter (m) of the pellet, and L is the length (m) of the pellet.

Durability

The drop resistance and deformation resistance of the biomass pellets were used to define the durability of the pellets. The drop resistance of the pellets was determined by dropping a 60-mm sample from a stationary position 2 m above a smooth floor (Cheng *et al.* 2018). The pellets, which had lengths > 25 mm during the first step, were dropped again. The experiment was repeated three times by dropping all the pellets that had lengths greater than 25 mm. The drop resistance was defined as the ratio between the mass with a final length of more than 25 mm and the original sample mass, according to GB/T15459 (1995).

The deformation resistance was tested using a universal pressure machine (WDW-10G; Tianchen Testing Machine Manufacturing Co., Ltd., Jinan, China). The pellets were horizontal placed in the center of the working table of the machine, and continuous loading force was applied to the feedstock at a speed of 10 mm/min until the pellet was broken. The computer will automatically record the peak value of force, which determined as the force of deformation resistance. The process was repeated five times and the value of maximum pressure was recorded each time (Lisowski *et al.* 2019).

Thermogravimetric Analysis

The combustion performance of the fuel pellets was analyzed using a synchronous thermal analyzer (STA 449 F5; Netzsch, Selb, Germany) including thermogravimetric (TG), derivative thermogravimetry (DTG), and differential scanning calorimetry (DSC). Approximately 25 ± 0.2 mg of each type of biomass fuel pellet was used for the analysis. Nitrogen was used as the protective gas with a flow rate of 20 mL/min, and temperature was raised from 30 °C to 1000 °C with a heating rate of 20 ºC/min.

The combustion characteristics of the 12%, 12%, 14% moisture content of SD, CS, PS were comprehensively analyzed, respectively. The ignition temperature (T_i) was defined using the method previously described by Chen *et al.* (2019). First, a vertical line was drawn through the peak point of the DTG curve to meet the TG curve. Secondly, the tangent of the TG curve was obtained at the point where the mass stopped changing. Finally, the temperature corresponding to the intersection point of the two tangents was obtained. The maximum burning rate (V_{max}) was calculated from the ordinate of the peak of the DTG curve. The peak temperature (T_m) was the temperature corresponding to the maximum weight loss rate (Peng *et al.* 2015). The burnout temperature (T_e) was the point where the tangent line intersected with l at the end of weightlessness of the TG curve (Chen *et al*. 2019). The ignition index (D_i) was determined using Eq. 3 (Xin *et al.* 2019).

$$D_i = V_{max} / (T_i T_m) = (d_w / d_t)_{max} / (T_i T_m) \quad (3)$$

In Eq. 3, V_{max} is the maximum burning rate (%/min), T_i is the ignition temperature (°C), and T_m is the temperature corresponding to the maximum mass loss rate (°C). The burnout index (D_e) was determined using Eq. 4 (Mureddu *et al.* 2018),

$$D_e = V_{max} / (\Delta t_{1/2} t_m t_e) \quad (4)$$

where $\Delta t_{1/2}$ is the time range of $(d_w / d_t) / (d_w / d_t)_{max} = 0.5$, t_m is the corresponding time of $(d_w / d_t)_{max}$ (min), and t_e is the burnout time (min). The flammability index (C) was determined using Eq. 5 (Tian and Liao 2013), and the comprehensive combustion characteristic index formula (S) was determined using Eq. 6 (Wang *et al.* 2018b),

$$C = V_{max} / T_i^2 \quad (5)$$

$$S = (V_{max} V_{mean}) / (T_i^2 T_e) \quad (6)$$

where V_{mean} is the average burning rate $(d_w / d_t)_{mean}$ (%/min), and T_e is the burnout temperature (°C).

RESULTS AND DISCUSSION

Biomass Characterization

The basic characteristics of all the three types of biomass pellets are presented in Table 2. It is clear from the table that SD had the highest volatile contents (79.2%) compared to the other two samples, but the fixed carbon contents of the SD was the lowest, *i.e.*, 11.4%. The nitrogen and sulfur contents of biomass were low, which means that burning these pellets causes lower emissions of NOx and SO_2 (Yao *et al.* 2017). In addition, the heating value of SD (19.1×10^6 J·kg^{-1}) was higher than CS (16.61×10^6 J·kg^{-1}) and PS (16.43×10^6 J·kg^{-1}). The SD showed heating values that were higher due to the lower moisture contents, as the presence of moisture in biomass reduces the energy availability from biomass (McKendry 2002).

Table 2. Proximate and Ultimate Analyses of Selected SD, CS, and PS Samples

Samples	Proximate Analysis (wt%)				Ultimate Analysis (wt%)					HV (MJ·kg^{-1})		
	M	V	FC	A	C	H	O	N	S	12%	14%	16%
SD	8.8	79.2	11.4	0.6	47.52	6.34	45.39	0.14	0	19.10	18.74	18.39
CS	10.2	66.2	14.8	8.8	41.97	5.80	42.21	1.12	0.06	16.61	16.36	16.01
PS	10.1	60.8	17.7	11.5	44.02	5.82	37.48	1.13	0.04	16.43	16.35	16.04

Physical Properties of Biomass Fuel Pellets

Appearance and microstructure

The appearance and microstructure of biomass fuel pellets for all three types of feedstock under different moisture contents are shown in Fig 2. Figure 2(A) shows the appearance of the feedstocks. The surfaces of SD, CS, and PS were smoother when prepared at 12%, 12%, and 14% moisture contents, respectively. The particles formed had cracks of varying degrees under other moisture contents, and a moisture content of 16% led to the most serious cracks. Figure 2(B) shows that the SD and CS prepared at 12% had flat and smooth compression structures, whereas SD and CS had slightly split structures at 14% moisture and obvious cracks at 16% moisture. The PS prepared at 14% showed smooth and textured compression. However, the PS had a negligible amount of cracks at 12% moisture; however, at 16% moisture it had a porous structure, as shown in Fig. 2(B). It is clear from the figure that the moisture contents of the feedstock played a remarkable role in the morphology as well as the pellet forming process. The reason for the development of the crack structure was that at higher temperatures, the water present in biomass was converted to steam, which caused cracks to appear in the pellets at higher moisture contents (Filbakk *et al.* 2011).

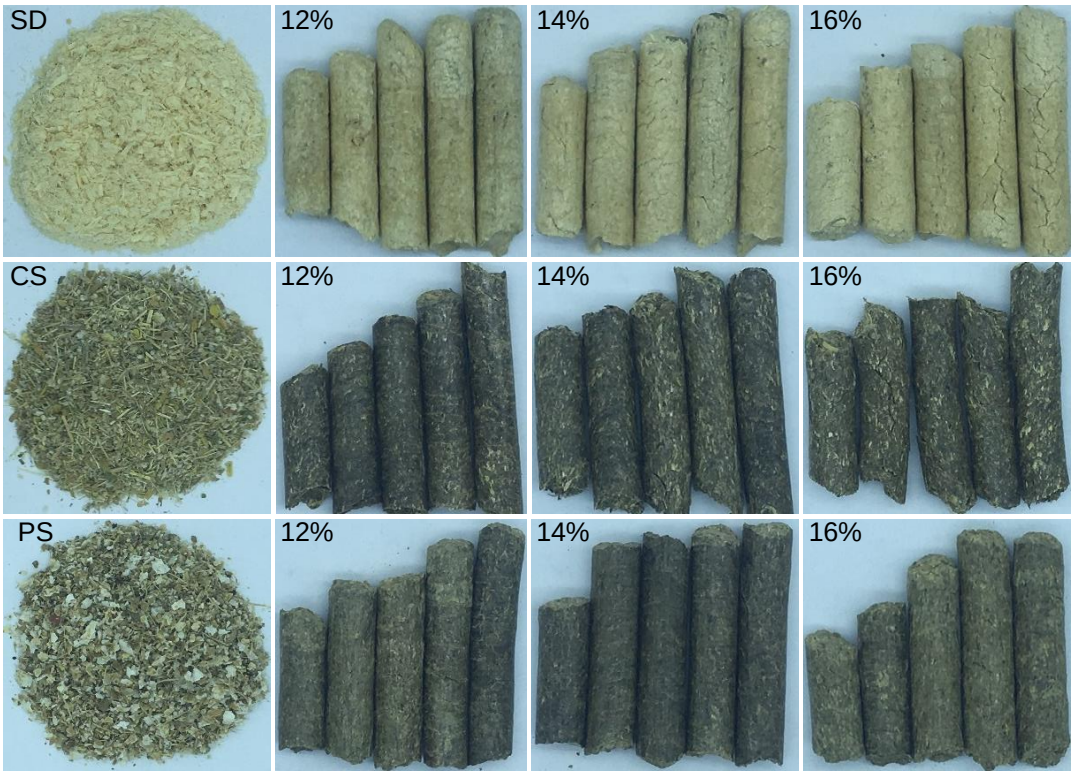

(A)

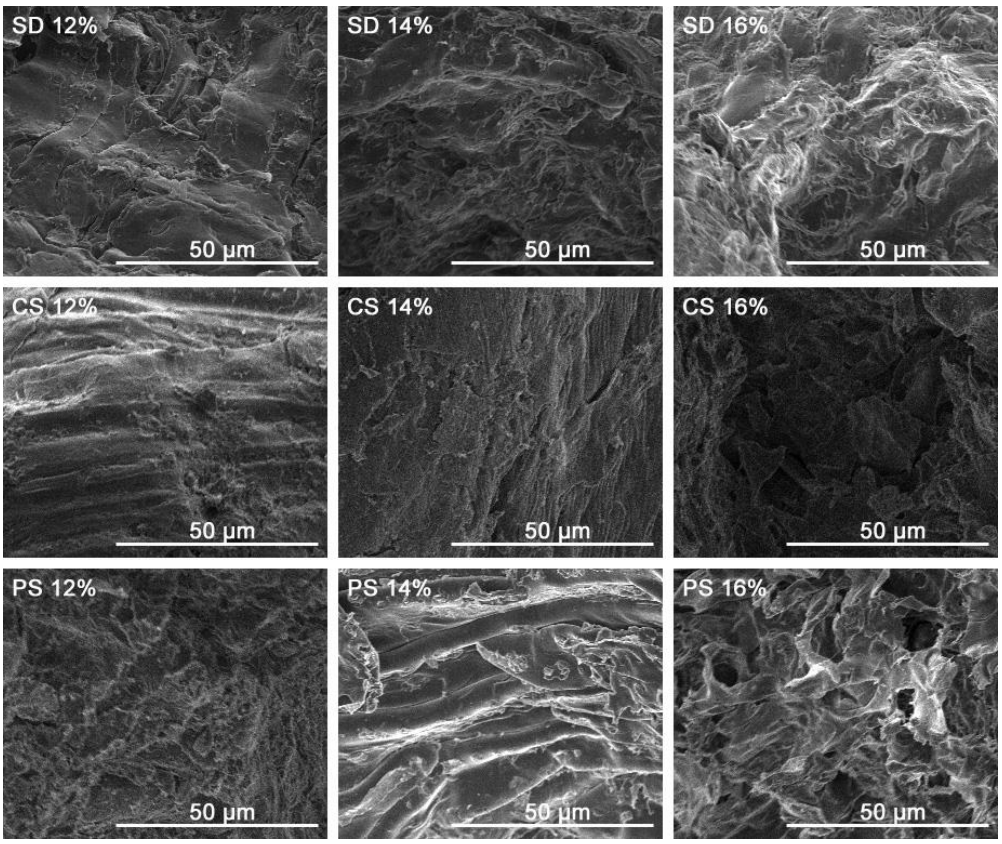

(B)

Fig. 2. (A) Appearance and morphology of fuel pellets at different levels of moisture SD, CS, and PS and (B) SEM images of SD, CS, and PS under different moisture contents

In contrast, the lower moisture contents of the feedstocks resulted in higher friction between the biomass and mold, causing the pellet forming process not to be smooth (Frodeson *et al.* 2019). The appearance and morphology of SD and CS was best at a moisture content of 12%, whereas PS showed better results at a moisture content of 14%. The results of the study were comparable with a previous study in which it was concluded that the densification process would improve with a moisture level in the range of 12% to 20% (Lisowski *et al.* 2017).

Pellet density

The pellet density of the fuel pellets for all types of feedstock under different conditions of moisture is presented in Fig. 3. It was clear that the molding process was greatly affected by moisture content. The pellet density of all the fuel pellets was greater than 1000 kg/m^3, which was comparable with the results of a previous study conducted by Huang *et al.* (2017). It was also clear from Fig. 3 that the relaxation density of the SD and CS pellets decreased as the moisture content of the feedstocks increased and that the trends of pellet density observed in the present study were comparable with the results of a previous study by Kaliyan and Vance Morey (2009a). However, the increase in the moisture content of feedstock initially resulted in an increase in the pellet density for PS pellets, and then decreased.

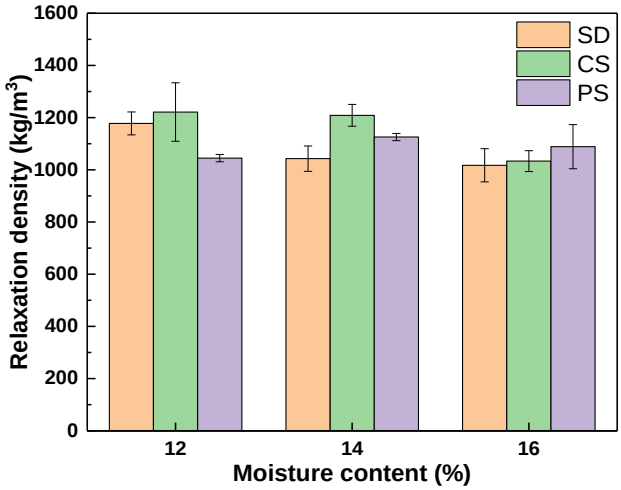

Fig. 3. Pellet density of biomass fuel pellets with different moisture content

The pellet density of SD and CS was highest at a moisture content of 12% with a value of 1180 kg/m^3 and 1220 kg/m^3, respectively. The value of the pellet density for SD and CS in this study was higher than previous studies in which palletization of SD was performed by a piston-type pelletizing machine at a moisture level of 9% to 13% and CS was pelletized by a flat die pelletizing machine at a moisture level of 30% to 33% (Lee *et al.* 2013; Tumuluru 2014). In contrast, the PS showed the highest value of pellet density at a moisture content of 14% with 1130 kg/m^3. The pellet density of PS was lower than the previous study by Fasina (2008) in which PS was pelletized using a single-pellet press at moisture contents of 5% to 20%. The maximum pellet density of the fuel pellets was initially found because the water present in the feedstock occupied the space between particles, which resulted in increased mass while the volume remained constant, causing the pellet density to increase. As the moisture contents of the feedstocks increased, the

extra water began to occupy the volume by sticking on the surface of the particles, affecting the bonding of the biomass particles and causing the density of the pellets to decrease. The density of the pellets decreased at higher moisture levels, *i.e.*, 16% because the extra moisture occupied the volume by increasing the resistance to compression, which resulted in a decrease in the pellet's strength and density (Huang *et al.* 2017). The results of the pellet density were consistent with appearance and morphology.

Drop resistance

The drop resistance of the fuel pellets is shown in Fig. 4. It was clear that the drop resistance of SD and CS decreased with the increase of moisture content. In contrast, the drop resistance of PS initially increased with the increase of moisture and then decreased at higher moisture contents. The maximum drop resistances were 80%, 97.02%, and 71.6% for SD, CS, and PS pellets at a moisture level of 12%, 12%, and 14%, respectively. The reason for the decrease in drop resistance of SD and CS with an increase in moisture level was consistent with the previous analysis of pellet density described earlier. The decrease for PS may have been due to its larger particle size than that of SD and CS after being crushed, as can be seen in Fig. 2(A). This caused it to require more water and immersion for it to play a binder role. When the moisture contents exceeded the optimal level, the extra water stacked on the surface of the particles prevented the formation of pellets, causing the drop resistance to decrease. The conclusion that moisture can be used as a binder was confirmed in previous studies as well (Puig-Arnavat *et al.* 2016; Frodeson *et al.* 2019).

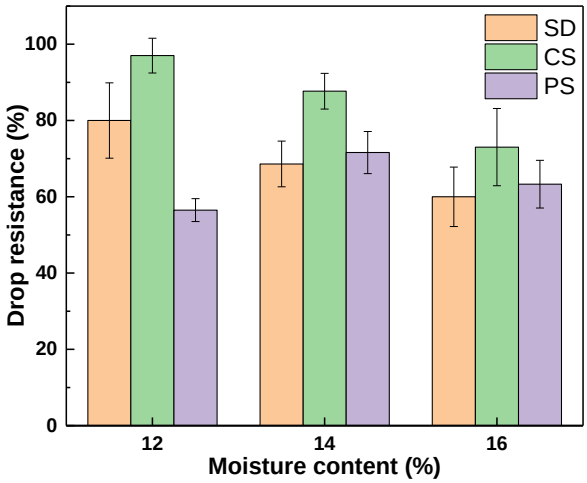

Fig. 4. Drop resistance of the biomass fuel pellets at different levels of moisture

Deformation resistance

The deformation resistance of pellets prepared from SD, CS, and PS with different moisture content is shown in Fig. 5. It was clear that the deformation resistance of the SD pellets was not affected by the increase in moisture content. However, the deformation resistance of the CS and PS pellets was remarkably affected by the moisture content. As presented in Fig. 5, the deformation resistance of the SD pellets remained constant with the increase of moisture with a value of approximately 0.4 KN ± 0.05 KN In contrast, the CS pellets showed the maximum deformation resistance (1.37 KN) at a moisture content of 12%. As the moisture contents of the feedstock increased, the deformation resistance

dropped to 0.42 KN at a moisture content of 14% and to 0.27 KN at a moisture content of 16%. The deformation resistance of the PS pellets was 0.32 KN at a moisture content of 12%. However, when the moisture was increased to 14%, the deformation resistance also increased up to 1.07 KN. With further increments in moisture content, the deformation resistances dropped to 0.28 KN. The reason for this phenomenon may be the more uniform particle size of SD compared to the other feedstocks as shown in Fig. 2(A), which allowed it to more easily combine with water. Moreover, the cascading structure of SD, as shown in Fig. 2(B) had sufficient axial force and a smaller radial force; thus, more moisture was required to encapsulate the role of lubrication promotion due to the larger particle size of the PS. When the moisture reached saturation levels, the extra water formed a water film, which increased the distance between particles and weakened the intermolecular forces of the particles, resulting in poor deformation resistance. The results of the deformation resistance were consistent with the pore structure as demonstrated by Fig. 2(B). The CS pellet had already reached optimal moisture levels, so the addition of extra water resulted in weak bonding of the particles with each other, leading to poor deformation resistance.

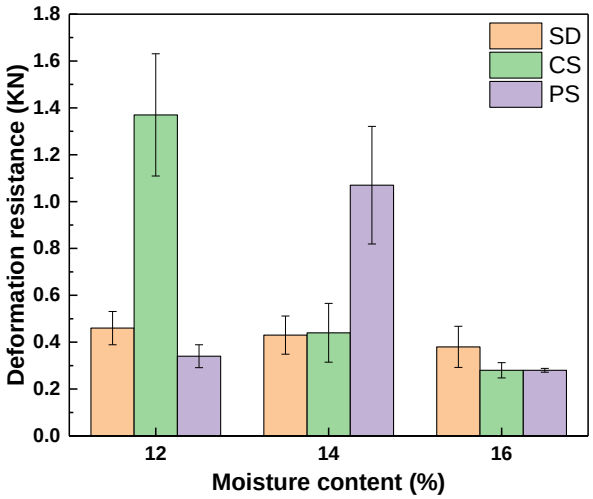

Fig. 5. Deformation resistance of biomass fuel pellets with different moisture contents

Thermogravimetric Experiment of Biomass Fuel Pellets

The combustion characteristics of all three types of fuel pellets were analyzed by comparing their thermogravimetric curves. The TG curves of all three types of fuel pellets are shown in Fig. 6. The TG curves of the three samples showed similar trends during combustion. The TG curve roughly consisted of three sequential stages designated as evaporation of moisture, combustion of volatile matter, and combustion of fixed carbon. During the first stage of combustion, from a temperature range of 30 °C to 175 °C, higher weight loss was observed for the PS pellets than that of the SD and CS pellets, which was consistent with the original moisture content of pellets. Moreover, the maximum weight loss for all types of pellets was observed in the temperature range of 175 °C to 400 °C. Overall, the SD pellets showed the highest weight loss profile, whereas the weight loss profile was lowest in PS pellets. This may have been due to the high volatiles content in the SD pellets (Gong *et al*. 2018). As shown in Fig. 6, the trend of the weight loss profile of fuel pellets was as follows: SD > CS > PS. The results were consistent with the conclusion of volatile content presented in Table 2. As the temperature increased beyond 400 °C, the weight loss was mainly caused by the combustion of fixed carbon (Gong *et al*.

2018). Therefore, it can be stated that the best physical properties of SD, CS, PS were obtained with moisture contents of 12%, 12%, and 14%, respectively, when using a pellet mill with horizontal and ring type dies.

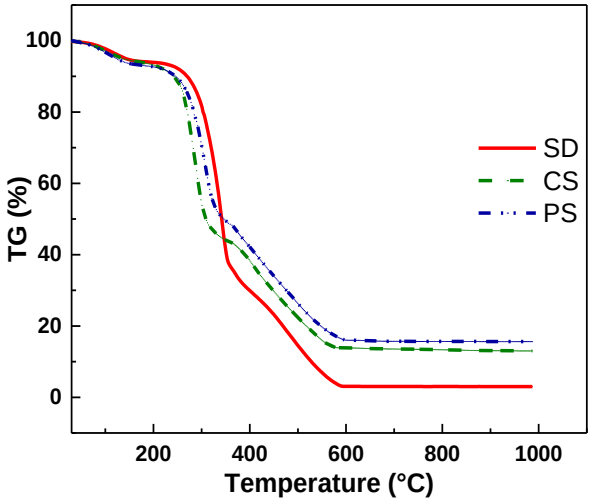

Fig. 6. TG curves of SD, CS, and PS fuel pellets

The DTG curves of all three types of fuel pellets are presented in Fig. 7. Two main peaks were observed in the DTG curve. The first peak was slight, which corresponded to the moisture evaporation stage of the TG curve (Chen *et al.* 2019). A strong peak appeared between the temperature range from 250 °C to 350 °C in the curve of the rate of weight loss.

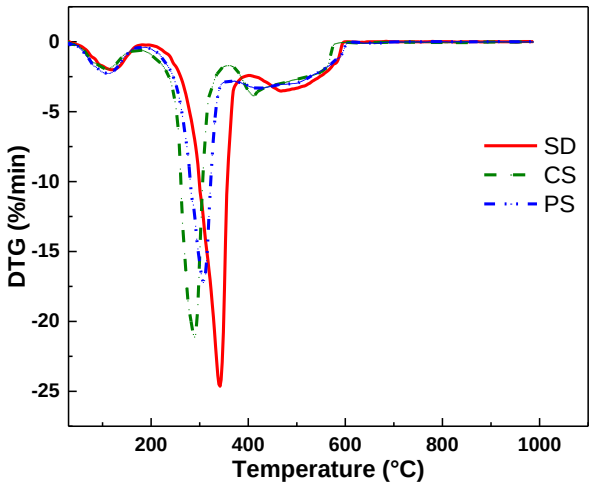

Fig. 7. DTG curves of SD, CS, and PS fuel pellets

The value of the weight loss rate for the SD pellets was 24.6%/min, while for the CS and PS pellets it was 21.1%/min and 17.2%/min, respectively, when the temperature was increased to 342 °C, 291 °C, and 308 °C, respectively. This was mainly because when the reaction temperature increased, the volatiles started to release and burn (Zhou *et al.* 2016a). However, the high ash contents of the material caused a layer to form on the surface

of the material during later stages of combustion, which hindered the contact between oxygen and the material, causing incomplete combustion of the material (Yao *et al.* 2017). The results were consistent with the conclusion of volatile content and the ash content presented in Table 2, and the peak size of the samples was consistent with the results of the second stage weight loss in Fig. 6 (Engin and Atakül 2018). During the last stage, the fixed carbon continuously decomposed at slower rates (Peng *et al.* 2015; Chen *et al.* 2019).

DSC curves are used to detect endothermic and exothermic reactions in the samples and to determine the combustion parameters such as peak temperature, ignition temperature, and burnout temperature (Mureddu *et al.* 2018). As shown in Fig. 8, it was observed that SD, CS, and PS pellets had an obvious exothermic peak within the temperature range of 400 °C to 600 °C. In addition, it was found that pellets made from CS had a smaller endothermic peak in the range of 300 °C to 400 °C, which may be because of the content of hemicellulose in CS is higher than other feedstocks (Zhou *et al.* 2016a; Bai *et al.* 2017). The SD heat release at peak duration temperature range was smaller than in PS; this was because of the fact that the volatile content of SD was higher and ash content was less, which eventually led to a faster combustion reaction rate in SD. The results of current study are consistent with a previous study that ash content had a certain hindrance to the combustion reaction (Engin and Atakül 2018).

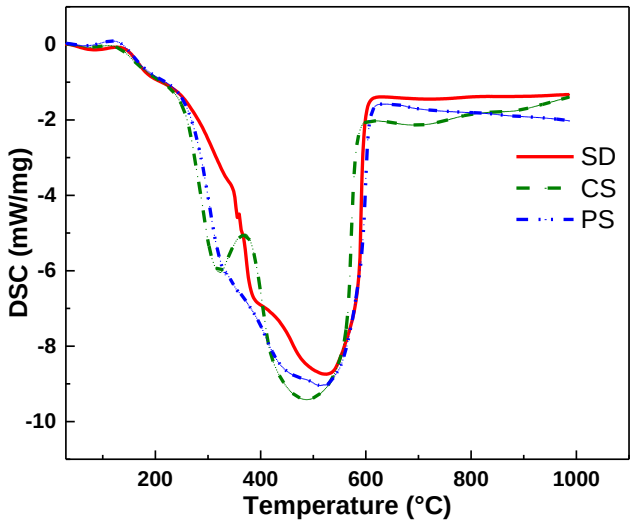

Fig. 8. DSC curves of SD, CS, and PS fuel pellets

Table 3 shows that in the absence of any additives, the ignition temperature (251 °C) of CS was the lowest compared with SD (296 °C) and PS (262 °C), which may be because CS reached the point of no further weight loss first when the temperature was low, and the volatile matter was released earlier, promoting its combustion (Riaza *et al.* 2017). These results were consistent with the previously described findings of DTG curves. Furthermore, the various combustion indexes of CS were higher compared to SD and PS. Moreover, the combustion performance of the samples were better with a higher value of S (Gong *et al.* 2018).

Table 3. Combustion Parameters of the Combustion of Different Biomass Fuel Pellets

Sample	T_i (°C)	T_e (°C)	$D_i \times 10^{-4}$	$D_e \times 10^{-3}$	$C \times 10^{-4}$	$S \times 10^{-7}$
SD	296	385	2.43	2.23	2.81	11.10
CS	251	346	2.89	2.51	3.35	14.05
PS	262	374	2.13	1.86	2.51	9.99

CONCLUSIONS

1. The basic characteristics studied by proximate and ultimate analysis showed that the volatile matter of pine sawdust (SD) was the highest, and the fixed carbon and ash of peanut shell (PS) were the highest, which had a remarkable effect on the combustion characteristics of the later stage. The moisture content affected the heating value of the pellets and lower moisture contents corresponded with higher heating value.
2. Through comparing the physical properties of the biomass pellets under different moisture contents, it was found that the density of all pellets was higher than 1000 kg/cm^3 and the drop resistance of the all the pellets was not considerably different. However, the deformation resistance of the samples under different moisture contents was quite different, and the appropriate moisture content can improve the deformation resistance of the samples. Therefore, the optimum moisture content of SD, corn straw (CS), and PS without a binder was 12%, 12%, and 14%, respectively. The moisture contents beyond the optimum value had a negative effect on the physical properties of the pellets.
3. Depending on the combustion parameters, the combustion performance of the CS pellets without addition of additives was the best, but emission analysis is necessary to ensure the clean combustion of fuels.

ACKNOWLEDGEMENTS

The authors appreciate that this work was financially supported by the National Key Research and Development Program of China (No. 2018YFD1101001), the Natural Science Foundation of Shandong Province of China (No. ZR2019MEE036), the Distinguished Expert of Taishan Scholars Shandong Province project, and the Higher Education Superior Discipline Team Training program of Shandong Province.

REFERENCES CITED

Bahrami, M., and Abbaszadeh, P. (2013). "An overview of renewable energies in Iran," *Renewable and Sustainable Energy Reviews* 24, 198-208. DOI: 10.1016/j.rser.2013.03.043

Bai, X. P., Wang, G. H., Gong, C. X., Yu, Y., Liu, W. N., and Wang, D. C. (2017). "Co-pelletizing characteristics of torrefied wheat straw with peanut shell," *Bioresource Technology* 233, 373-381. DOI: 10.1016/j.biortech.2017.02.091

Bajwa, D. S., Peterson, T., Sharma, N., Shojaeiarani, J., and Bajwa, S. G. (2018). "A review of densified solid biomass for energy production," *Renewable and Sustainable Energy Reviews* 96, 296-305. DOI: 10.1016/j.rser.2018.07.040

China National Energy Administration (2016). "Thirteen five year plan of biomass," (http://zfxxgk.nea.gov.cn/auto87/201612/t20161205_2328.htm?keywords=), Accessed 17 June 2019.

Chen, C. X., Qin, S. H., Chen, F., Lu, Z. G., and Cheng, Z. (2019). "Co-combustion characteristics study of bagasse, coal and their blends by thermogravimetric analysis," *Journal of the Energy Institute* 92(2), 364-369. DOI: 10.1016/j.joei.2017.12.008

Cheng, J., Zhou, F., Si, T., Zhou, J., and Cen, K. (2018). "Mechanical strength and combustion properties of biomass pellets prepared with coal tar residue as a binder," *Fuel Processing Technology* 179, 229-237. DOI: 10.1016/j.fuproc.2018.07.011

Colley, Z., Fasina, O. O., Bransby, D., and Lee, Y. Y. (2006). "Moisture effect on the physical characteristics of switchgrass pellets," *Transactions of the ASABE* 49(6), 1845-1851. DOI: 10.13031/2013.22271

Demirbas, A. (2004). "Combustion characteristics of different biomass fuels," *Progress in Energy and Combustion Science* 30(2), 219-230. DOI: 10.1016/j.pecs.2003.10.004

Engin, B., and Atakül, H. (2018). "Air and oxy-fuel combustion kinetics of low rank lignites," *Journal of the Energy Institute* 91(2), 311-322. DOI: 10.1016/j.joei.2016.11.004

Fasina, O. O. (2008). "Physical properties of peanut hull pellets," *Bioresource Technology* 99(5), 1259-1266. DOI: 10.1016/j.biortech.2007.02.041

Filbakk, T., Skjevrak, G., Høibø, O., Dibdiakova, J., and Jirjis, R. (2011). "The influence of storage and drying methods for Scots pine raw material on mechanical pellet properties and production parameters," *Fuel Processing Technology* 92(5), 871-878. DOI: 10.1016/j.fuproc.2010.12.001

Florentino-Madiedo, L., Díaz-Faes, E., García, R., and Barriocanal, C. (2018). "Influence of binder type on greenhouse gases and PAHs from the pyrolysis of biomass briquettes," *Fuel Processing Technology* 171, 330-338. DOI: 10.1016/j.fuproc.2017.11.029

Frodeson, S., Henriksson, G., and Berghel, J. (2019). "Effects of moisture content during densification of biomass pellets, focusing on polysaccharide substances," *Biomass and Bioenergy* 122, 322-330. DOI: 10.1016/j.biombioe.2019.01.048

GB/T 15459 (1995). "Method for determination of crushing strength of coal," Standardization Administration of China, Beijing, China.

GB/T 28731 (2012). "Proximate analysis of solid biofuels," Standardization Administration of China, Beijing, China.

Gil, M. V., Oulego, P., Casal, M. D., Pevida, C., Pis, J. J., and Rubiera, F. (2010). "Mechanical durability and combustion characteristics of pellets from biomass blends," *Bioresource Technology* 101(22), 8859-8867. DOI: 10.1016/j.biortech.2010.06.062

Gong, Z. Q., Wang, L., Wang, Z. B., Wang, Z. T., Xu, Y., Sun, F. Q., Sun, Z. Q., Liu, Z. Z., and Zhu, L. Y. (2018). "Experimental study on combustion and pollutants emissions of oil sludge blended with microalgae residue," *Journal of the Energy Institute* 91(6), 877-886. DOI: 10.1016/j.joei.2017.10.001

Gu, H. D., Tang, Y. Z., Yao, J., and Chen, F. (2019). "Study on biomass gasification under various operating conditions," *Journal of the Energy Institute* 92(5), 1329-1336. DOI: 10.1016/j.joei.2018.10.002

Guo, M. X., Song, W. P., and Jeremy, B. (2015). "Bioenergy and biofuels: History, status, and perspective," *Renewable and Sustainable Energy Reviews* 42, 712-725. DOI: 10.1016/j.rser.2014.10.013

Huang, Y., Finell, M., Larsson, S., Wang, X., Zhang, J., Wei, R., and Liu, L. (2017). "Biofuel pellets made at low moisture content – Influence of water in the binding mechanism of densified biomass," *Biomass and Bioenergy* 98, 8-14. DOI: 10.1016/j.biombioe.2017.01.002

JJG 017 (1996). "Ultimate analysis of solid biofuels," Standardization Administration of China, Beijing, China.

Kaliyan, N., and Vance Morey, R. (2009a). "Densification characteristics of corn stover and switchgrass," *Transactions of the ASABE* 52(3), 907-920. DOI: 10.13031/2013.21202

Kaliyan, N., and Vance Morey, R. (2009b). "Factors affecting strength and durability of densified biomass products," *Biomass and Bioenergy* 33(3), 337-359. DOI: 10.1016/j.biombioe.2008.08.005

Khan, A. A., De Jong, W., Jansens, P. J., and Spliethoff, H. (2009). "Biomass combustion in fluidized bed boilers: Potential problems and remedies," *Fuel Processing Technology* 90(1), 21-50. DOI: 10.1016/j.fuproc.2008.07.012

Lam, P. S. W., Sokhansanj, S., Bi, X., Lim, J. C., Naimi, L. J., Hoque, M., Mani, S., Womac, A. R., Ye, X. P., and Narayan, S. (2008). "Bulk density of wet and dry wheat straw and switchgrass particles," *Applied Engineering in Agriculture* 24(3), 351-358. DOI: 10.13031/2013.24490

Lee, S. M., Ahn, B. J., Choi, D. H., Han, G.-S., Jeong, H.-S., Ahn, S. H., and Yang, I. (2013). "Effects of densification variables on the durability of wood pellets fabricated with *Larix kaempferi* C. and *Liriodendron tulipifera* L. sawdust," *Biomass and Bioenergy* 48, 1-9. DOI: 10.1016/j.biombioe.2012.10.015

Li, H., Liu, X. H., Legros, R., Bi, X. T., Lim, C. J., and Sokhansanj, S. (2012). "Pelletization of torrefied sawdust and properties of torrefied pellets," *Applied Energy* 93, 680-685. DOI: 10.1016/j.apenergy.2012.01.002

Lisowski, A., Dąbrowska-Salwin, M., Ostrowska-Ligęza, E., Nawrocka, A., Stasiak, M., Świętochowski, A., Klonowski, J., Sypuła, M., and Lisowska, B. (2017). "Effects of the biomass moisture content and pelleting temperature on the pressure-induced agglomeration process," *Biomass and Bioenergy* 107, 376-383. DOI: 10.1016/j.biombioe.2017.10.029

Lisowski, A., Pajor, M., Świętochowski, A., Dąbrowska, M., Klonowski, J., Mieszkalski, L., Ekielski, A., Stasiak, M., and Piątek, M. (2019). "Effects of moisture content, temperature, and die thickness on the compaction process, and the density and strength of walnut shell pellets," *Renewable Energy* 141, 770-781. DOI: 10.1016/j.renene.2019.04.050

Longhin, E., Gualtieri, M., Capasso, L., Bengalli, R., Mollerup, S., Holme, J. A., Øvrevik, J., Casadei, S., Benedetto, C. D., Parenti, P., *et al.* (2016). "Physico-chemical properties and biological effects of diesel and biomass particles," *Environmental Pollution* 215, 366-375. DOI: 10.1016/j.envpol.2016.05.015

Mani, S., Tabil, L. G., and Sokhansanj, S. (2003). "An overview of compaction of biomass grinds," *Powder Handling and Processing* 15(3), 160-168.

McKendry, P. (2002). "Energy production from biomass (part 1): Overview of biomass," *Bioresource Technology* 83(1), 37-46. DOI: 10.1016/S0960-8524(01)00118-3

Mureddu, M., Dessì, F., Orsini, A., Ferrara, F., and Pettinau, A. (2018). "Air- and oxygen-blown characterization of coal and biomass by thermogravimetric analysis," *Fuel* 212, 626-637. DOI: 10.1016/j.fuel.2017.10.005

Obernberger, I., and Thek, G. (2004). "Physical characterisation and chemical composition of densified biomass fuels with regard to their combustion behavior," *Biomass and Bioenergy* 27(6), 653-669. DOI: 10.1016/j.biombioe.2003.07.006

Peng, X. W., Ma, X. Q., and Xu, Z. B. (2015). "Thermogravimetric analysis of co-combustion between microalgae and textile dyeing sludge," *Bioresource Technology* 180, 288-295. DOI: 10.1016/j.biortech.2015.01.023

Puig-Arnavat, M., Shang, L., Sárossy, Z., Ahrenfeldt, J., and Henriksen, U. B. (2016). "From a single pellet press to a bench scale pellet mill — Pelletizing six different biomass feedstocks," *Fuel Processing Technology* 142, 27-33. DOI: 10.1016/j.fuproc.2015.09.022

Riaza, J., Gibbins, J., and Chalmers, H. (2017). "Ignition and combustion of single particles of coal and biomass," *Fuel* 202, 650-655. DOI: 10.1016/j.fuel.2017.04.011

Saidur, R., Abdelaziz, E. A., Demirbas, A., Hossain, M. S., and Mekhilef, S. (2011). "A review on biomass as a fuel for boilers," *Renewable and Sustainable Energy Reviews* 15(5), 2262-2289. DOI: 10.1016/j.rser.2011.02.015

Sokhansanj, S., Mani, S., Bi, X. T., Zaini, P., and Tabil, L. G. (2005). "Binderless pelletization of biomass," in: *ASAE 2005 Annual International Meeting Tampa*, Tampa, FL, USA, pp. 1-13.

Tian, H., and Liao, Z. Z. (2013). "Combustion characteristics and combustion kinetics of agriculture biomass," *Transactions of the Chinese Society of Agricultural Engineering* 29(10), 203-212. (In Chinese with English abstract). DOI: 10.3969/j.issn.1002-6819.2013.10.028

Tumuluru, J. S., Wright, C. T., Hess, J. R., and Kenney, K. L. (2011). "A review of biomass densification systems to develop uniform feedstock commodities for bioenergy application," *Biofuels, Bioproducts and Biorefining* 5(6), 683-707. DOI: 10.1002/bbb.324

Tumuluru, J. S. (2014). "Effect of process variables on the density and durability of the pellets made from high moisture corn stover," *Biosystems Engineering* 119, 44-57. DOI: 10.1016/j.biosystemseng.2013.11.012

Trubetskaya, A., Leahy, J. J., Yazhenskikh, E., Müller, M., Layden, P., Johnson, R., Ståhl, K., and Monaghan, R. F. D. (2019). "Characterization of woodstove briquettes from torrefied biomass and coal," *Energy* 171, 853-865. DOI: 10.1016/j.energy.2019.01.064

Verma, V. K., Bram, S., Vandendael, I., Laha, P., Hubin, A., and De Ruyck, J. (2011). "Residential pellet boilers in Belgium: Standard laboratory and real life performance with respect to European standard and quality labels," *Applied Energy* 88(8), 2628-2634. DOI: 10.1016/j.apenergy.2011.02.004

Wang, Y., Wu, K., and Sun, Y. (2018a). "Effects of raw material particle size on the briquetting process of rice straw," *Journal of the Energy Institute* 91(1), 153-162. DOI: 10.1016/j.joei.2016.09.002

Wang, Q., Wang, G. W., Zhang, J. L., Lee, J.-Y., Wang, H. Y., and Wang, C. (2018b). "Combustion behaviors and kinetics analysis of coal, biomass and plastic," *Thermochimica Acta* 669, 140-148. DOI: 10.1016/j.tca.2018.09.016

Xin, S. Z., Huang, F., Liu, X. Y., Mi, T., and Xu, Q. L. (2019). "Torrefaction of herbal medicine wastes: Characterization of the physicochemical properties and combustion

behaviors," *Bioresource Technology* 287, Article ID 121408. DOI: 10.1016/j.biortech.2019.121408

Yao, Z. L., Ma, X. Q., Wang, Z. H., and Chen, L. M. (2017). "Characteristics of co-combustion and kinetic study on hydrochar with oil shale: A thermogravimetric analysis," *Applied Thermal Engineering* 110, 1420-1427. DOI: 10.1016/j.applthermaleng.2016.09.063

Zhou, C. C., Liu, G. J., Wang, X. D., and Qi, C. C. (2016a). "Co-combustion of bituminous coal and biomass fuel blends: Thermochemical characterization, potential utilization and environmental advantage," *Bioresource Technology* 218, 418-427. DOI: 10.1016/j.biortech.2016.06.134

Zhou, Y. G., Zhang, Z. X., Zhang, Y. X., Wang, Y. G., Yu, Y., Ji, F., Ahmad, R., and Dong, R. J. (2016b). "A comprehensive review on densified solid biofuel industry in China," *Renewable and Sustainable Energy Reviews* 54, 1412-1428. DOI: 10.1016/j.rser.2015.09.096

Article submitted: October 2, 2019; Peer review completed: November 17, 2019; Revised version received: November 22, 2019; Accepted: November 23, 2019; Published: December 3, 2019.
DOI: 10.15376/biores.15.1.557-573